Dalton Transactions

COMMUNICATION

View Article Online
View Journal | View Issue

Cite this: *Dalton Trans.*, 2019, **48**, 11647

Received 22nd May 2019,
Accepted 9th July 2019

DOI: 10.1039/c9dt02159k

rsc.li/dalton

Exceptionally slow magnetic relaxation in a mononuclear hexacoordinate Ni(II) complex†

Ján Titiš, *[a] Veronika Chrenková,[a] Cyril Rajnák,[a] Ján Moncol,[b] Dušan Valigura[a] and Roman Boča[a]

A hexacoordinate mononuclear $[Ni(pydm)_2](dnbz)_2$ complex shows field-induced slow magnetic relaxation with two or three relaxation channels that are strongly supported by an external magnetic field. At B_{DC} = 0.8 T and T = 1.9 K, the low-frequency (LF) relaxation time is as slow as τ(LF) = 1.3 s with the mole fraction of x(LF) = 0.47.

Some complexes made up of the first transition metals are examples of systems showing field-induced slow magnetic relaxation (SMR) as a prerequisite of single-ion magnets (SIMs).[1] There are many cases of V, Cr, Mn, Fe, Co, Ni, and Cu in various oxidation states exhibiting such properties.[2,3] The most numerous class of SIMs is represented by Co(II) systems with two to eight coordination. On the other hand, the SIM behaviour of Ni(II) systems was confirmed only in a few complexes: hexacoordinate $[Ni(pydc)(pydm)]\cdot H_2O$, $[Ni(NCS)_2(nqu)_2(H_2O)_2]\cdot 2nqu$, and pentacoordinate $[Ni(mdabco)_2Cl_3]ClO_4$.[3] These are field-induced SIMs with significant negative magnetic anisotropy (D < 0). Multiple relaxation modes are operative in these systems, while the complex $[Ni(NCS)_2(nqu)_2(H_2O)_2]\cdot 2nqu$ exhibits one of the longest relaxation times in the low-frequency range (τ(LF) = 275 ms at T = 1.9 K and B_{DC} = 0.4 T). An increase in the DC field to B_{DC} = 1.2 T causes a prolongation of the time to 336 ms. The large negative value of the axial zero-field splitting parameter is no longer a necessary condition for SMR/SIM behaviour, since the systems with a positive and/or negligible value of D that show field-supported SMR are also known nowadays.[4]

The present study is devoted to a mononuclear Ni(II) complex of the composition $[Ni(pydm)_2](dnbz)_2$, hereafter **1**; pydm – 2,6-pyridinedimethanol and dnbz – 3,5-dinitrobenzoato(1-). X-ray structure analysis (Tables S1–S3 and Fig. S3–S5 in the ESI†) confirms that the central Ni(II) atom is hexacoordinate, with a $\{NiO_4N_2\}$ donor set resembling a compressed tetragonal bipyramid (Fig. 1).‡ This is a structural analogue of the previously reported Co(II) complex $[Co(pydm)_2](dnbz)_2$, hereafter **2**, which exhibits a long relaxation time at low temperature: τ(LF) = 0.13 s at B_{DC} = 0.4 T and T = 1.9 K.[5]

The DC susceptibility data were acquired using a SQUID magnetometer (Quantum Design, model MPMS-XL7) by applying B = 0.1 T. A correction to the underlying magnetism has been applied to raw data and then the molar susceptibility has been transformed to the temperature dependence of the effective magnetic moment. The magnetization data were obtained at two temperatures, T = 2.0 and 4.6 K, for the magnetic induction increasing up to B = 7.0 T.

The temperature dependence of the effective magnetic moment shows features typical of hexacoordinate Ni(II) complexes: a linear dependence on cooling and then a drop to a constant limit at the lowest temperatures. A slope reflects some temperature-independent paramagnetism (Fig. 2). The room temperature value of $\mu_{eff} = 3.49\mu_B$ gradually decreases on cooling to T = 15 K and then it decreases to $\mu_{eff} = 2.34\mu_B$ at T = 1.9 K. The magnetization per formula unit at T = 2.0 K and B = 7.0 T has a value of $M_1 = M_{mol}/\mu_B = 1.74$ that is far from the

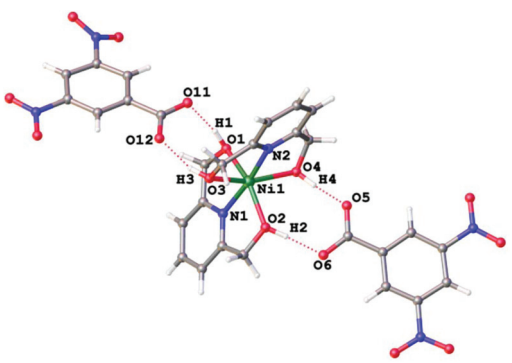

Fig. 1 Molecular structure of **1**.

[a]*Department of Chemistry, Faculty of Natural Sciences, University of SS Cyril and Methodius, 91701 Trnava, Slovakia. E-mail: roman.boca@ucm.sk*
[b]*Institute of Inorganic Chemistry, FCHPT, Slovak University of Technology, 812 37 Bratislava, Slovakia*

†Electronic supplementary information (ESI) available: Synthesis, spectra, X-ray structure data, and AC susceptibility data. CCDC 1915427. For ESI and crystallographic data in CIF or other electronic format see DOI: 10.1039/c9dt02159k

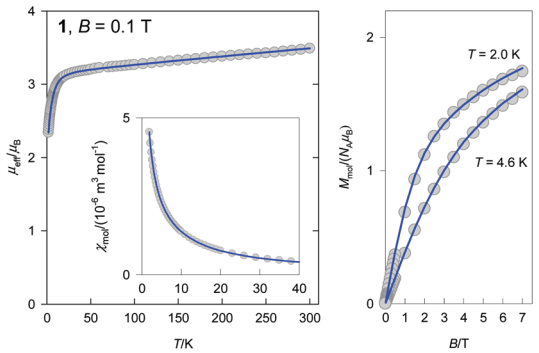

Fig. 2 DC magnetic functions for **1**. Solid lines – fitted by the zero-field splitting model.

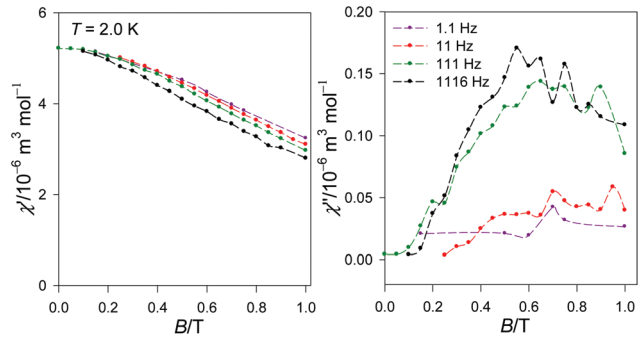

Fig. 3 AC susceptibility data for **1**: field dependence for a set of frequencies at T = 2.0 K.

spin-only value. Such behaviour indicates a considerable and negative value of the axial zero-field splitting parameter D.

The experimental data of susceptibility and magnetization were fitted simultaneously using a joint functional $F = w{\cdot}E(\chi) + (1 - w){\cdot}E(M)$; it balances the relative errors of susceptibility and magnetization, respectively.§

The spin-Hamiltonian of the form

$$\hat{H}_a^{\text{eff}} = D(\hat{S}_z^2 - \vec{S}^2/3)\hbar^{-2} + \mu_B B(g_z\hat{S}_z\cos\theta_a + g_{xy}\hat{S}_x\sin\theta_a)\hbar^{-1} \quad (1)$$

has been used, which contains the axial zero-field splitting parameter and the Zeeman term. The latter depends upon the orientation of the magnetic field for a number of grids distributed uniformly over the meridian (a = 16 for a quarter of the meridian). The eigenvalues of the above Hamiltonian are substituted to the formulae of statistical thermodynamics for susceptibility and magnetization, respectively. The fitting procedure based upon minimization of the error functional gave the following set of magnetic parameters: D/hc = −15.4 cm^{-1}, g_z = 2.50 and g_{xy} = 2.06; the additional corrections include the temperature-independent (para)magnetism, χ_{TIM} = 12 × 10^{-9} m^3 mol^{-1}, and the molecular field correction, zj/hc = −0.17 cm^{-1}. The quality of the fit measured by the discrepancy factors $R(\chi)$ = 0.0015 and $R(M)$ = 0.013 is excellent. Since the fit gave rather large g-factor anisotropy, we have also tested the situation with isotropic g (Fig. S6 in the ESI†). However, the fit in this case is slightly worse.

The magnetic parameters were also calculated by an *ab initio* CASSCF/NEVPT2 method.[6] Calculations gave the D-parameter in good agreement with that obtained by fitting the magnetic data: D_{calc}/hc = −14.65 cm^{-1} and E/D = 0.09; $\boldsymbol{g}$ {2.197, 2.219, and 2.321} and g_{iso} = 2.245. The contributions to D_{calc} are detailed in the ESI.†

The AC susceptibility data were obtained with the same hardware as the DC data, using the amplitude of the oscillating field B_{AC} = 0.38 mT. Different scans of the in-phase (χ') and out-of-phase (χ'') components were obtained by selecting the temperature, external DC magnetic field B_{DC}, and frequency f of the AC field.¶ The field dependence of the AC susceptibility response at T = 2.0 K for a set of representative frequencies is shown in Fig. 3. At the zero DC field, the out-of-phase susceptibility χ'' vanishes due to a fast magnetic relaxation. At the applied DC field, it passes through a maximum and then decreases at higher fields. This behaviour indicates that **1** shows a slow magnetic relaxation; this is field and frequency-dependent.

A more detailed AC response is shown in Fig. 4, where the AC susceptibility components are plotted as a function of the frequency f for a set of fields B_{DC} = 0.2 to 1.0 T, at a fixed T = 1.9 K. The data confirm a massive dependence of the out-of-phase susceptibility component on the applied external field. Two relaxation domains are well separated: the low-frequency (LF) relaxation process proceeds at f = 0.15 Hz, which implies that the relaxation time is $\tau = 1/(2\pi f)$ = 1.1 s. The high-frequency (HF) relaxation channel occurs at about f = 1000 Hz, yielding τ = 1.6 × 10^{-4} s at T = 1.9 K. In-between the intermediate-frequency (IF) channel is also evidenced.

The external DC field causes a prolongation of the LF relaxation time, since the peaks of the LF branch are moved to lower frequencies. Also, the height of the LF peak is supported by the applied field, so that the mole fraction of the LF species increases. At B_{DC} = 1.0, the relaxation time is τ(LF) = 1.2 s and

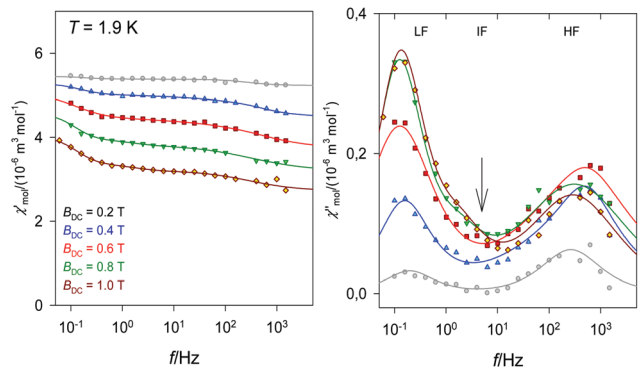

Fig. 4 AC susceptibility data for **1**: frequency dependence for a set of external fields at T = 1.9 K. Solid lines – fitted with a two- or three-set Debye model.

the mole fraction is x(LF) = 0.52. Such a long relaxation time for a mononuclear Ni(II) complex is an unexpected challenge.

The magnetic data (23 points for χ' and 23 points for χ'') were fitted to the extended three-set Debye model, as explained in the ESI.† The retrieved sets of the relaxation parameters (the isothermal susceptibilities χ_{Tk}, the distribution parameters α_k and the relaxation times τ_k for each k-th relaxation channel, along with the adiabatic susceptibility χ_S), Table 1, were used in the reconstruction of the interpolation/extrapolation lines that are shown in Fig. 4.

The frequency dependence of the AC susceptibility components for a set of temperatures at B_{DC} = 0.6 T is shown in Fig. 5. The LF relaxation domain is represented by a stable set of data points as opposed to the HF one showing some scattering.¶ The data fitting for the LF domain is well characterized by the set of magnetic parameters as proved by their standard deviations (Tables S5 and S6 in the ESI†). At the out-of-phase susceptibility, the heights of the LF and HF domains are approximately the same and they survive above 4.3 K. This is a rather unusual feature, since, as a rule, the LF domain escapes more rapidly with temperature. There is only a slight shift in the peak maximum for the LF relaxation domain, and consequently τ(LF) is little temperature-dependent.

A prolongation of the LF relaxation time for **1** [τ(LF) = 1.05 s at B_{DC} = 0.4 T and T = 1.9 K] relative to its isostructural analogue [Co(pydm)$_2$](dnbz)$_2$ [τ(LF) = 0.13 s at B_{DC} = 0.4 T and T = 1.9 K][4] is a surprise. Note the differences in the calculated spin-Hamiltonian parameters: [D_{calc}/hc = −14.65 cm^{-1}, E/D = 0.09, and g{2.197, 2.219, 2.321}] for **1** and [D_{calc}/hc = −94.8 cm^{-1}, E/D = 0.12, and g{1.975, 2.153, 3.073}] for **2**. For **2**, moreover, the application of the spin-Hamiltonian formalism is problematic due to the quasi-degeneracy causing a divergence of the perturbation theory because $D_i = 1/E_i$. The first excited triplet term in **2** is close lying, $E_{0\to1}$ = 447 cm^{-1}, and invokes an overestimation of the first contribution $D_{0\to1}$ = −104 cm^{-1}; in **1**, $E_{0\to1}$ = 7258 cm^{-1} and consequently $D_{0\to1}$ = −58 cm^{-1}. The axial zero-field splitting parameter D enters the barrier to spin reversal $U = |D|S^2$ when the Orbach relaxation mechanism applies. The present compound **1**, however, does not show the features of the Orbach mechanism for the HF relaxation channel at low temperature (Fig. S7 in the ESI†).

In conclusion, we have prepared a hexacoordinate Ni(II) complex with a significantly negative zero-field splitting parameter D. This complex shows a slow magnetic relaxation in a small DC magnetic field, with probably three relaxation channels. Despite D < 0, the Orbach mechanism is not operative in this case. At B_{DC} = 0.8 T and T = 1.9 K, the low-frequency relaxation time is τ(LF) = 1.3 s, which is the slowest value in the class of proven Ni(II) SIMs (Table S7 in the ESI†).

Table 1 Field dependence of the relaxation times τ_k and the mole fractions x_k for **1** at T = 1.9 K

B_{DC}/T	τ_{LF}/s	$\tau_{IF}/10^{-3}$ s	$\tau_{HF}/10^{-6}$ s	x_{LF}	x_{IF}	x_{HF}
0.2	0.82(35)	—	599	0.30	—	0.70
0.4	1.05(12)	0.29	798	0.33	0.21	0.46
0.6	1.29(24)	0.27	398	0.45	0.05	0.50
0.8	1.30(14)	83	503	0.47	0.07	0.46
1.0	1.22(43)	82	536	0.52	0.10	0.38

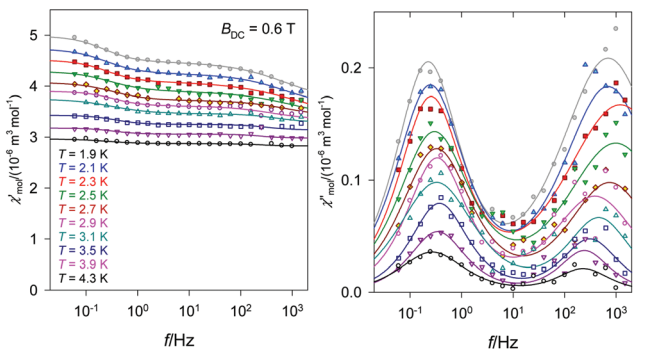

Fig. 5 Frequency dependence of the AC susceptibility components of **1** for a set of temperatures at B_{DC} = 0.6 T. Solid lines – fitted with a two-set Debye model.

Conflicts of interest

There are no conflicts to declare.

Acknowledgements

Slovak grant agencies (APVV 16-0039, APVV 18-0016, VEGA 1/0919/17 and VEGA 1/0013/18) are acknowledged for financial support. Also, the project NFP313010V954 of call OPVaI-VA/DP/2018/1.1.3-07 and the ITMS project 26240220084 co-founded by the European Regional Development Fund are acknowledged.

Notes and references

‡Crystallographic data: A single crystal of **1** was mounted on a Stoe StadiVari diffractometer possessing a PILATUS3R 300 K detector and a microfocused sealed tube Xenocs Genix3D Cu HD (λ = 1.54186 Å) at 100 K. The structure of **1** was solved using SUPERFLIP and refined using SHELXL (ver. 2018/3).[7,8] The structure was drawn using OLEX2 and MERCURY 4.0 programs.[9] Crystal data for **1**: $C_{28}H_{24}N_6NiO_{16}$, triclinic $P\bar{1}$, a = 7.9708(2), b = 13.7985(4), c = 14.6800(4) Å, α = 96.452(2), β = 103.366(2), γ = 100.715(2) deg, V = 1522.94(7) Å^3, Z = 2, D_c = 1.656 g cm^{-3}, μ = 1.733 mm^{-1}, F(000) = 780, T = 100(1) K, $2\theta_{max}$ = 142.306° (−9 ≤ h ≤ 6, −15 ≤ k ≤ 16, −18 ≤ l ≤ 16). Final results (461 parameters and 0 restraints): R_1 = 0.0308 and wR_2 = 0.0799 [$I > 2\sigma(I)$], and R_1 = 0.0316, wR_2 = 0.0805 and S = 1.052 for all 25 529 reflections. CCDC reference number 1915427.† CrystalExplorer[10] was used to calculate the Hirshfeld surface and associated fingerprint plots (see the ESI†).[11]

§ $F = w(1/n)\left[\sum_i^n \frac{|\chi_i^o - \chi_i^c|}{\chi_i^o}\right] + (1-w)(1/m)\left[\sum_j^m \frac{|M_j^o - M_j^c|}{M_j^o}\right]$, w = 0.8.

¶Technical note: Some AC susceptibility data are seriously scattered owing to a small amplitude of the AC field and a weak signal arising from the S = 1 spin system. The fluctuations of the DC magnetic field increase the possible scattering as well. Each experimental point results from an average of ten scans (averaging four blocks) with the omission of data outside 0.8σ interval.

1 (*a*) D. Gatteschi, R. Sessoli and J. Villain, *Molecular nanomagnets*, Oxford University press, 2006, pp. 1–408; (*b*) G. A. Craig and M. Murrie, *Chem. Soc. Rev.*, 2015, **44**, 2135; (*c*) S. Gómez-Coca, D. Aravena, R. Morales and E. Ruiz, *Coord. Chem. Rev.*, 2015, **289–290**, 379; (*d*) J. M. Frost, K. L. M. Harriman and M. Murugesu, *Chem. Sci.*, 2016, **7**, 2470; (*e*) M. Feng and M.-L. Tong, *Chem. – Eur. J.*, 2018, **24**, 7574.

2 (*a*) W. Lin, T. Bodenstein, V. Mereacre, K. Fink and A. Eichhofer, *Inorg. Chem.*, 2016, **55**, 2091; (*b*) R. C. Poulten, M. J. Page, A. G. Algarra, J. L. Le Roy, I. Lopez, E. Carter, A. Llobet, S. A. Macgregor, M. F. Mahon, D. M. Murphy, M. Murugesu and M. K. Whittlesey, *J. Am. Chem. Soc.*, 2013, **135**, 13640; (*c*) M. Atzori, L. Tesi, E. Morra, M. Chiesa, L. Sorace and R. Sessoli, *J. Am. Chem. Soc.*, 2016, **138**, 2154; (*d*) M. Ding, G. E. Cutsail, D. Aravena, M. Amoza, M. Rouzières, P. Dechambenoit, Y. Losovyj, M. Pink, E. Ruiz, R. Clérac and J. M. Smith, *Chem. Sci.*, 2016, **7**, 6132; (*e*) R. Boča, C. Rajnák, J. Titiš and D. Valigura, *Inorg. Chem.*, 2017, **56**, 1478.

3 (*a*) J. Miklovič, D. Valigura, R. Boča and J. Titiš, *Dalton Trans.*, 2015, **44**, 12484; (*b*) D. Lomjanský, J. Moncoľ, C. Rajnák, J. Titiš and R. Boča, *Chem. Commun.*, 2017, **53**, 6930; (*c*) K. E. R. Marriott, L. Bhaskaran, C. Wilson, M. Medarde, S. T. Ochsenbein, S. Hill and M. Murrie, *Chem. Sci.*, 2015, **6**, 6823.

4 C. Rajnák, J. Titiš, J. Moncol, R. Mičová and R. Boča, *Inorg. Chem.*, 2019, **58**, 991.

5 D. Valigura, C. Rajnák, J. Moncol, J. Titiš and R. Boča, *Dalton Trans.*, 2017, **46**, 10950.

6 (*a*) F. Neese, The ORCA program system, *Wiley Interdiscip. Rev.: Comput. Mol. Sci.*, 2012, **2**, 73; (*b*) F. Neese, *ORCA – An Ab Initio, Density Functional and Semi-empirical Program Package, Version 4.0.0*; (*c*) M. Atanasov, D. Ganyushin, D. A. Pantazis, K. Sivalingam and F. Neese, *Inorg. Chem.*, 2011, **50**, 7460; (*d*) C. Angeli, S. Borini, M. Cestari and R. Cimiraglia, *J. Chem. Phys.*, 2004, **121**, 4043; (*e*) C. Angeli, R. Cimiraglia, S. Evangelisti, T. Leininger and J.-P. Malrieu, *J. Chem. Phys.*, 2001, **114**, 10252; (*f*) C. Angeli, R. Cimiraglia and J.-P. Malrieu, *J. Chem. Phys.*, 2002, **117**, 9138; (*g*) F. Neese, *J. Chem. Phys.*, 2005, **122**, 34107; (*h*) D. Ganyushin and F. Neese, *J. Chem. Phys.*, 2006, **125**, 24103; (*i*) F. Neese, *J. Chem. Phys.*, 2007, **127**, 164112.

7 L. Palatinus and G. Chapuis, *J. Appl. Crystallogr.*, 2007, **40**, 786.

8 G. M. Sheldrick, *Acta Crystallogr., Sect. C: Struct. Chem.*, 2015, **71**, 3.

9 (*a*) O. V. Dolomanov, L. J. Bourhis, R. J. Gildea, J. A. K. Howard and H. Puschmann, *J. Appl. Crystallogr.*, 2009, **42**, 339; (*b*) C. F. Macrae, I. J. Bruno, J. A. Chisholm, P. R. Edgington, P. McCabe, E. Pidcock, L. Rodriquez-Monge, R. Taylor, J. van de Streek and P. A. Wood, *J. Appl. Crystallogr.*, 2008, **41**, 466.

10 M. J. Turner, J. J. McKinnon, S. K. Wolf, D. J. Gromwood, P. R. Spackman, D. Jayalitaka and M. A. Spackman, *CrystalExplored17.5*, The University of Western Australia, 2017.

11 (*a*) M. A. Spackman and D. Jayalitaka, *CrystEngComm*, 2009, **11**, 19; (*b*) M. A. Spackman and J. J. McKinnon, *CrystEngComm*, 2002, **4**, 378.